AJNR

MR Features of Diseases Involving Bilateral Middle Cerebellar Peduncles

Kouichirou Okamoto, Susumu Tokiguchi, Tetsuya Furusawa, Kazuhiro Ishikawa, Akther F. Quardery, Satoru Shinbo and Keisuke Sasai

AJNR Am J Neuroradiol 2003, 24 (10) 1946-1954
http://www.ajnr.org/content/24/10/1946

AJNR Am J Neuroradiol 24:1946–1954, November/December 2003

MR Features of Diseases Involving Bilateral Middle Cerebellar Peduncles

Kouichirou Okamoto, Susumu Tokiguchi, Tetsuya Furusawa, Kazuhiro Ishikawa, Akther F. Quardery, Satoru Shinbo, and Keisuke Sasai

BACKGROUND AND PURPOSE: **Distribution of lesions or involvement of specific anatomic sites can suggest the diagnosis of disease. The purpose of this study was to investigate what diseases affect both middle cerebellar peduncles (MCPs) and to evaluate other MR features for differential diagnosis.**

METHODS: **MR findings of 27 patients (14 male and 13 female; age range, 4–77 years [mean, 48.5 years]) with bilateral MCP lesions were retrospectively studied.**

RESULTS: **Neurodegenerative diseases were the most frequent diagnoses (n = 11 [41%]: sporadic olivopontocerebellar atrophy, eight; Shy-Drager syndrome, one; spinocerebellar ataxia, two). Also included were metabolic diseases (n = 6 [22%]: adrenoleukodystrophy, two; Wilson disease, two; cirrhosis of the liver, one; and hypoglycemia, one); cerebrovascular diseases, including posterior reversible encephalopathy syndrome (n = 3 [11%]: infarction, one; hypertensive encephalopathy, one; cyclosporin-A encephalopathy, one), demyelinating and inflammatory diseases (n = 4 [15%]: multiple sclerosis, one; acute disseminated encephalomyelitis, one; Behçet disease, one; and HIV encephalopathy, one), and neoplasms (n = 3 [11%]: lymphoma, one; glioma, one; meningeal carcinomatosis, one). All patients showed symmetrical T2 hyperintensity in both MCPs, except for one with malignant lymphoma. Marked atrophy in the posterior fossa was characteristically seen in neurodegenerative diseases. Enlargement of the pons was observed in hypertensive encephalopathy and neoplasms but absent in meningeal carcinomatosis. Lesions were restricted in the posterior fossa in eight patients with neurodegenerative diseases and one with brain stem glioma. Other patients had supratentorial lesions.**

CONCLUSION: **Symmetricity of MCP lesions, morphologic change of the posterior fossa structures, and distribution of other lesions are helpful in the differential diagnosis.**

MR imaging is the most sensitive imaging technique to depict brain lesions as altered signal intensities. Most of the lesions are demonstrated as hyperintensities on T2-weighted MR images, and the signal intensity itself is nonspecific. Characteristic distribution of lesions or involvement of specific anatomic sites, however, can suggest the diagnosis or narrow the differential diagnosis.

The middle cerebellar peduncle (MCP) consists of the transversely coursing pontocerebellar fibers that arch across the midline and gather on each side (1). The MCPs can be evaluated by routine MR examination, and normal MCPs show homogeneous white matter signal intensity. Bilateral involvement of the MCPs is well known in olivopontocerebellar atrophy (OPCA) (2) but is relatively rare in other diseases. We retrospectively reviewed the MR findings and the clinical charts of the patients with bilateral MCP lesions to investigate what disorders affect both MCPs and to evaluate other MR features for differential diagnosis. A literature review on bilateral involvement of MCPs is also presented.

Methods

MR reports at our university hospital were reviewed to identify patients with bilateral involvement of the MCPs between January 1994 and March 2003.

There were 27 patients: 14 male and 13 female, ranging in age from 4 to 77 years (mean, 48.5 years). MR images were obtained with 1.5T MR units (Magnetom H-15 and Vision, Siemens, Erlangen, Germany; and Signa Horizon Lx Echospeed, General Electric Medical Systems, Milwaukee, WI).

Received May 15, 2003; accepted after revision June 23.

From the Department of Radiology, Niigata University Faculty of Medicine (K.O., T.F., K.I., A.F.Q., K.S.), Niigata City, Japan, Department of Neurology, Ojiya General Hospital (S.T.), Ojiya City, Japan, and Department of Neurology, Kawase Neurology Clinic (S.S.), Sanjo City, Japan.

Part of this work was presented at the 62nd Annual Meeting of the Japan Radiological Society, Yokohama, Japan, April 11–13, 2003.

Address correspondence to K. Okamoto, MD, Department of Radiology, Niigata University Faculty of Medicine, 1–757 Asahi-machi-dori, Niigata 951-8510, Japan.

Axial T1-weighted spin-echo (SE) (490–600/9–15/1–2 [TR/TE/NEX]) and T2-weighted SE (3000/90/1) or fast SE (FSE) images (3000–3600/96–102/2) with echo train lengths of five or 10 were obtained in all patients. The section thickness was 6 mm; intersection gap, 1 mm; field of view, 220–230 mm; and matrix, 256 × 256 mm. Contrast material (gadopentetate dimeglumine 0.1 mmol/kg) was used in 20 patients. Diffusion-weighted images ($b = 1000$ s/mm^2) were obtained for 16 patients. Coronal T2-weighted FSE images were obtained for nine patients.

An additional patient, a 70-year-old woman with leukodystrophy, showed bilateral MCP involvement. This patient was not included in this study because of unknown pathologic cause. Without coronal T2-weighted images, it was difficult to evaluate T2 signal intensity of extremely atrophic MCPs on axial-plane images because partial volume phenomenon of high signal intensity from CSF surrounding atrophic MCPs could not be eliminated. Two such patients with sporadic OPCA (sOPCA) were excluded from this study.

Results

Diseases classified as neurodegenerative are the most frequent in this series (n = 11 [41%]: sOPCA, eight; Shy-Drager syndrome [SDS], one; and spinocerebellar ataxias, two), although diagnoses of the patients were varied. Also included were metabolic diseases (n = 6 [22%]: adrenoleukodystrophy [ALD], two; Wilson disease, two; alcoholic cirrhosis of the liver, one; and hypoglycemic coma, one); cerebrovascular diseases, including posterior reversible encephalopathy syndrome (n = 3 [11%]: anterior inferior cerebellar artery (AICA) infarction, one; hypertensive encephalopathy, one; and cyclosporin-A encephalopathy, one), demyelinating and inflammatory diseases (n = 4 [15%]: multiple sclerosis [MS], one; acute disseminated encephalomyelitis [ADEM], one; Behçet disease, one; and HIV encephalopathy, one), and malignant neoplasms (n = 3 [11%]: malignant lymphoma, one; brain stem glioma, one; and meningeal carcinomatosis, one). Diagnoses of spinocerebellar ataxias (SCA2 and SCA6) were confirmed by genetic analysis with the patients' consent. Diagnoses of malignant neoplasms were confirmed with biopsy or autopsy. Other diseases were diagnosed on the basis of clinical and laboratory findings.

All patients showed symmetrical hyperintensity in both MCPs except for one with diffusely infiltrating malignant lymphoma. MR imaging revealed additional infra- or supratentorial abnormal signal intensities or both were found in all patients. A patient with alcoholic cirrhosis of the liver and a patient with hypoglycemic coma had no pontine lesion on T2-weighted images, but small symmetrical hyperintensities along the bilateral pyramidal tracts were observed in the basal portion of the pons on diffusion-weighted images in the hypoglycemic patient. Other patients showed T2 hyperintensities in the pons.

Three of eight patients with sOPCA showed bilateral linear hyperintensity at the lateral margin of the atrophic putamen. The remaining eight patients with neurodegenerative diseases and a patient with brain stem glioma had no supratentorial lesions, but various supratentorial lesions were observed in the other patients.

Marked atrophy of the pons, MCPs, and cerebellum was seen in all patients with neurodegenerative diseases, except for one with SDS. Milder atrophy of these structures was seen in patients with ALD or Wilson disease. Mild cerebellar atrophy was seen in a patient with MS. On the other hand, enlargement of the pons and cerebellum with extensive T2 hyperintensity was seen in a patient with hypertensive encephalopathy. Two patients with neoplasms (malignant lymphoma and brain stem glioma) showed enlargement of the pons; however, enlargement of the affected brain stem and MCPs was absent in a mildly hydrocephalic patient with meningeal carcinomatosis.

No MCP lesions showed contrast enhancement after the administration of gadopentetate dimeglumine. Gadolinium enhancement was seen in two patients with neoplasms: a case of glioma with a pontine lesion of the brain stem and that of meningeal carcinomatosis showing leptomeningeal enhancement. No gadolinium enhancement in diffusely infiltrating malignant lymphoma existed.

Diagnoses and MR features of the patients are summarized in the Table.

Discussion

Bilateral symmetrical hyperintensity of both MCPs at T2-weighted imaging is a well-known MR finding in patients with OPCA (2). In the present study, bilateral T2 hyperintensity of the MCPs was most frequently seen in patients with neurodegenerative diseases, including OPCA. In addition, it was observed in various pathologic conditions: metabolic diseases; cerebrovascular diseases, including posterior reversible encephalopathy syndrome; neoplasms; and inflammatory and demyelinating diseases.

Neurodegenerative Diseases

sOPCA is the largest group in this study. In OPCA, the bilateral symmetrical hyperintensity on T2-weighted images is characteristically seen in the atrophic MCPs with high frequency (2, 3). This hyperintensity represents lack of histologic staining of the myelin of the transverse pontine fibers (2). Similar symmetrical, but subtle T2 hyperintensity of the MCPs was observed in SDS. sOPCA, SDS, and striatonigral degeneration (SND) are major clinical subtypes of multiple system atrophy (MSA), and MR findings observed in sOPCA can be seen in SDS and SND with lower frequency, and vice versa (3). Three of eight patients with sOPCA showed bilateral linear hyperintensity at the lateral margin of the atrophic putamen (2), which is more frequently seen in SND (3).

Similar symmetrical T2 hyperintense signal intensity of both MCPs was observed in spinocerebellar ataxias (SCA2 and SCA6) (Fig 1). SCAs are autosomal dominant cerebellar ataxias (ADCAs), in which many types have been identified by molecular genetic assignment. On the other hand, ADCA has been

Diseases involving bilateral middle cerebellar peduncles

Diagnosis (no.)	Age/sex	Pontine Lesions	Cbll Lesions	Other Lesions
Degenerative diseases (11)				
sOPCA (8)	47, 50, 53, 55/M, 61, 68, 71, 72/F	Cross sign, atrophy	Atrophy	Atrophy of basal ganglia with linear hyperintensity at lateral margins (3)
SCA2 (1)	42/M	Cross sign, atrophy	Atrophy	(-)
SCA6 (1)	48/F	Cross sign, atrophy	Atrophy	(-)
Shy-Drager synd (1)	57/M	Linear lesion on midline	(-)	(-)
Metabolic diseases (6)				
Adrenoleukodystrophy (2)	4, 38/M	Lesions along pyramidal tracts (1), heterogeneous lesions (1),	WML (2)	Large symmetrical parieto-occipial WML (1), lesions along pyramidal tracts (1)
Wilson disease (2)	24/M, 34/F	Several small lesions (2), atrophy (1)	Mild atrophy (1)	Midbrain (tegmentum) and basal ggl lesions (2) and thalamic lesions (1)
Alcoholic liver cirrhosis (1)	51/M	(-)	Mild atrophy	T1 hyperintensity at globi pallidi
Hypoglycemic coma (1)	52/F	Lesions along pyramidal tracts on DWI	(-)	Hyperintensity lesions along pyramidal tracts on T2WI and DWI
Neoplasms (3)				
Diffuse infiltrating ML (1)	55/F	Heterogeneous lesions, enlargement	Diffuse WML	Whole corpus callosum and diffuse cbr WML
Brain stem glioma (1)	74/M	Ring-enhancement, enlargement	(-)	Tumor extension into medulla oblongata and midbrain
Meningeal carcinomatosis (1)	77/F	Multiple lacunar infarcts	Enhancement in fissures	Leptomeningeal enhancement, multiple lacunar infarction, mild hydrocephalus
Cerebrovascular disease, hypertensive and its related encephalopathies (3)				
AICA infarction (1)	57/M	Lacunar infarcts	Infarction in AICA distribution	Multiple lacunar infarction
Hypertensive encephalopathy (1)	51/F	Heterogeneous lesion, enlargement	Diffuse WML, swelling	Midbrain, basal ganglia, thalamus, bilateral hippocampus, periventricular WML
Cyclosporin-A encephalopathy (1)	16/F	A few punctate lesions	Diffuse swelling	Small parietal WML
Inflammatory & demyelinating diseases (4)				
Multiple sclerosis (1)	17/F	Small tegmental lesions	Mild atrophy	Small lesions in corpus callosum, small oval periventricular WML
ADEM (1)	38/M	Heterogeneous lesions	(-)	Multiple subcortical WML
Behcet disease (1)	66/F	Subtle heterogeneous lesions	(-)	Non-specific punctate WML
HIV encephalopathy (1)	31/M	Diffuse hyperintensity	(-)	Frontal WML, mild brain atropohy
Total (27)	mean age, 48.5 y			

Note.—ADEM, acute disseminated encephalomyelitis; cbll, cerebellar; cbr, cerebral; DWI, diffusion-weighted imaging; ggl, ganglia; HIV, human immunodeficiency virus; ML, malignant lymphoma; SCA, spinocerebellar ataxia; sOPCA, sporadic olivopontocerebellar atrophy; T2WI, T2-weighted imaging; WML, white matter lesions.

recently separated into three clinical subtypes (ADCA-I, -II, and -III). ADCA-I, the most common subtype, is characterized by supranuclear ophthalmoplegia, optic atrophy, basal ganglia symptoms, dementia, and amyotrophy (4). Genetic heterogeneity of ADCA-I has been established with disease loci assigned to chromosome 6p (SCA1), 12q (SCA2), 14q (SCA3/Machado-Joseph disease), and 16q (SCA4). SCA2 is characterized by marked OPCA (4, 5). The leading symptoms of patients with SCA6 are compatible with ADCA-III, which is characterized by a pure cerebellar syndrome (6); however, the condition of some patients with SCA6 can be clinically diagnosed as sOPCA (6). MR findings of our SCA patients (SCA2 and SCA6) were identical with those of sOPCA without basal ganglia lesions. Characteristic T2 hyperintense "cross sign" in the pons, which was thought to be a typical feature of MSA (5), was observed in all of our sOPCA patients and SCA patients, and marked atrophy of the brain stem and cerebellum was also demonstrated. Therefore, differentiation of such SCA2 and SCA6 from sOPCA pa-

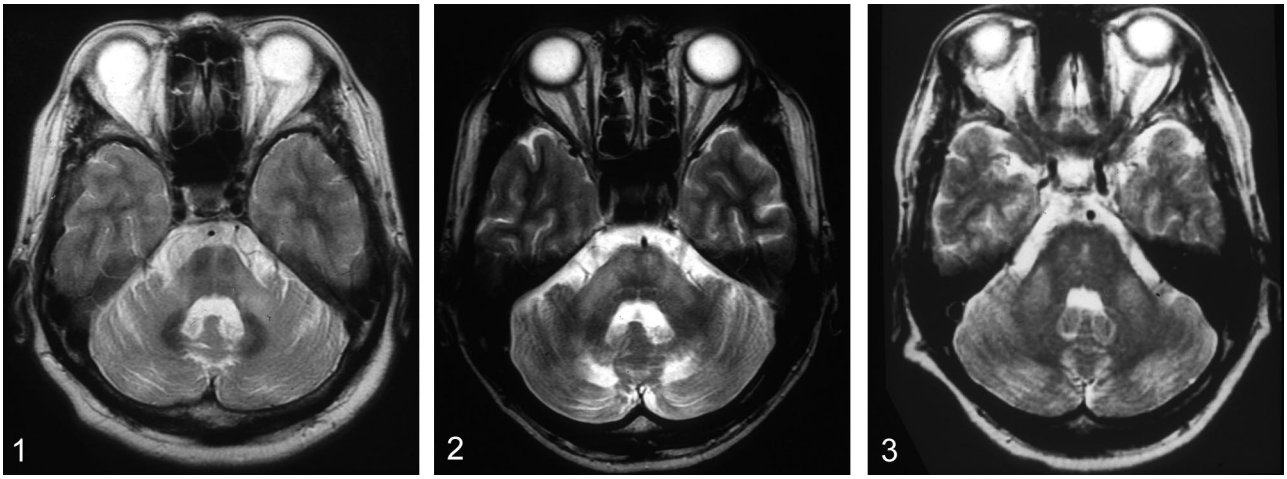

FIG 1. A 48-year-old woman with spinocerebellar ataxia (SCA6). T2-weighted fast spin-echo (FSE) MR image (3,600/102/2) shows bilateral symmetrical hyperintensity of atrophic MCPs. The pons with the "cross sign" and cerebellum are also atrophic. These MR findings are identical to that of sOPCA.

FIG 2. A 38-year-old man with ALD. T2-weighted FSE MR image (3,600/102/2) shows bilateral symmetrical hyperintensity of both MCPs, pyramidal tracts in the pons, and cerebellar white matter. The cerebellum is atrophic, and the fourth ventricle is slightly dilated.

FIG 3. A 34-year-old woman with Wilson disease. T2-weighted FSE MR image (3,600/102/2) shows symmetrical bilateral hyperintensity in both MCPs. There are several small hyperintensities in the pons. Mild atrophy of the cerebellum is seen.

tients is impossible on the basis of MR imaging. The cross sign reflects degeneration of pontine neurons and transverse pontocerebellar fibers in various types of olivopontocerebellar atrophy, irrespective of the underlying pathogenetic process (5). Although the cross sign has also been reported in SCA3/Machado-Joseph disease (5, 7), mild atrophy of the cerebellum and brain stem is distinct from typical OPCA (4). In addition, the hyperintensity in both MCPs has not been mentioned in SCA3 cases. During this study, four patients with SCA3/Machado-Joseph disease underwent MR examination, but no patient showed T2 hyperintensity in the MCPs. In an autopsy case of SCA3, the pontine nuclei, transverse fibers, and upper and MCPs showed considerable atrophy associated with nerve cell loss, but without gliosis, demyelination, or change of neuronal density (8). Lack of gliosis and demyelination may explain the absence of MCP hyperintensity in SCA3.

No patients with dentatorubral-pallidoluysian atrophy (DRPLA) were included in this study, but similar T2 hyperintensity has been reported in senile-onset DRPLA patients (9). DRPLA is an autosomal dominant neurodegenerative disorder characterized by variable combinations of myoclonus, epilepsy, cerebellar ataxia, choreathetosis, and dementia, as well as the demonstration of an expanded CAG trinucleotide repeat on chromosome 12p (9). T2-weighted MR images show characteristically symmetrical hyperintense lesions in the cerebral white matter, globus pallidus, thalamus, midbrain, and pons, as well as bilateral MCPs with brain atrophy in senile-onset DRPLA (9).

Symmetrical hyperintensity in the atrophic MCPs with atrophy of the brain stem and cerebellum is characteristic of neurodegenerative disorders.

Metabolic Diseases

Patients with ALD (Fig 2), Wilson disease (Fig 3), alcoholic cirrhosis of the liver, or hypoglycemic coma (Fig 4) showed the symmetrical hyperintensity in both MCPs. Mild cerebellar atrophy was seen in ALD, Wilson disease, and alcoholic cirrhosis of the liver.

ALD is an X-linked disorder that involves mainly the nervous system white matter, the adrenal cortex, and the testes. It is associated with the abnormal accumulation of very long saturated fatty acids in the brain and adrenal gland, red blood cells, and plasma, attributable to impaired capacity of peroxisomes to degrade them. Cerebral white matter abnormalities consist of diffuse loss of myelin with mild gliosis and many perivascular periodic acid-Schiff-positive cells. Cerebellar involvement is common. The phenotypic expression of ALD varies widely (10). One of our patients presented as the childhood cerebral phenotype with characteristic MR demonstration of large symmetric areas in the parietal and occipital white matter, extending across the splenium of the corpus callosum, and the other presented as the adult neurologic variant, adrenomyeloneuropathy, with brain abnormalities limited to long tracts (10). Bilateral symmetrical T2 hyperintensity, however, was commonly seen in the MCPs and cerebellar white matter in both ALD patients. Hyperintense lesions were also demonstrated in the pons.

Wilson disease, or hepatolenticular degeneration, is an inborn error of copper metabolism that is characterized by an inability of the liver to excrete copper into the bile (11, 12). It is well known that there is a predilection for involvement of the outer rim of the putamen and ventral nuclear mass of the thalami, but the midbrain, substantia nigra, red nuclei, inferior tectum, crura, pons, and cerebellum are also affected

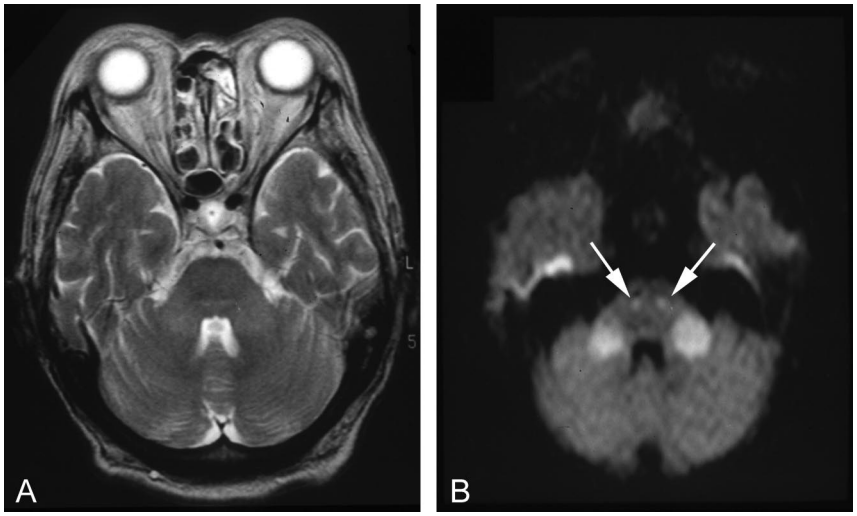

FIG 4. A 60-year-old woman with hypoglycemic coma. *A,* T2-weighted FSE MR image (3,600/102/2) on admission shows subtle symmetrical hyperintensity in both MCPs. *B,* Isotropic diffusion-weighted MR image (b = 1,000 s/mm^2) obtained at the same time shows markedly hyperintense signal intensity in both MCPs. In addition, small symmetrical hyperintensities along the pyramidal tracts are demonstrated (*arrows*). These hyperintensities disappeared completely on repeated MR imaging performed the next day (not shown).

with involvement of the superior and MCPs (11, 12). Involvement of bilateral MCPs is not emphasized in Wilson disease, but the symmetrical hyperintensity in both MCPs has been demonstrated in some patients on MR imaging (11, 12). One of two patients with Wilson disease showed atrophic change of the pons, MCPs, and cerebellum as well as bilateral symmetrical linear T2 hyperintensity at the lateral margin of the atrophic putamen, and these characteristics were similar to those of MSA. The atrophy was milder in the posterior fossa, however, and the cross sign was absent in the pons. In addition, heterogeneously T2 hyperintense lesions in the medial thalami and midbrain observed in the patient with Wilson disease are not demonstrated in MSA. MR similarity with Wilson disease is reported in patients with acquired hepatocerebral degeneration with chronic hepatic diseases (13, 14), and symmetrical hyperintensities have been demonstrated in the bilateral MCPs and putamina in a patient with liver cirrhosis on T2-weighted MR images (14). In our alcoholic patient with cirrhosis of the liver, the hyperintense signal in both MCPs was subtle on axial T2-weighted images, but the increased signal intensity was confirmed on coronal T2-weighted images. In patients with portosystemic shunt, characteristic hyperintensity was seen in the globus pallidus bilaterally on T1-weighted images (11, 15). Additional symmetrical T1 hyperintensity can be seen in the thalami in Wilson disease (12).

Subtle symmetrical hyperintensity was seen in both MCPs on axial T2-weighted images in our hypoglycemic patient, but the lesions were markedly hyperintense on isotropic diffusion-weighted imaging with b value of 1000 s/mm^2. No increased signal intensity was visualized on T2-weighted images, but additional hyperintensities were observed along the bilateral pyramidal tracts on diffusion-weighted imaging. The patient became alert promptly after the intravenous administration of glucose, and the lesions disappeared completely on an MR examination obtained the next day. Symmetrical MR abnormal signal intensities have been reported in the caudate and lenticular nuclei, cerebral cortex, substantia nigra, or hippocampus after onset of hypoglycemic coma (16, 17). In a case of uncomplicated hypoglycemic coma, subtle hyperintensity of bilateral MCPs was demonstrated on MR imaging performed 3 days after admission, but the authors did not mention the finding (17). Hyperintensities on diffusion-weighted images have been demonstrated bilaterally in the basal ganglia, hippocampus, and cerebral cortex in a hypoglycemic patient with poor outcome (18). Hyperintensities of both MCPs and pyramidal tracts on diffusion-weighted images and their rapid resolution without sequelae, however, have not been documented so far.

Bilateral symmetrical MCP lesions have been reported in the late phase of Tay-Sachs disease, also called "infantile GM2 gangliosidosis," with diffuse hyperintense lesions in the cerebral and cerebellar white matter on T2-weighted images. Severe brain atrophy and hyperintensity in the basal ganglia, thalamus, and cerebral cortex have been demonstrated on T1-weighted images (19).

Cerebrovascular Disease and Posterior Reversible Encephalopathy Syndrome

Cerebrovascular diseases affect bilateral MCPs primarily and secondarily. Although infarction isolated to the AICA territory is by far the rarest of those in the cerebellum, the MCP can be involved (20–22). Bilateral MCP infarction was demonstrated in our patient with simultaneous cerebellar infarcts in AICA distributions (Fig 5). Atherosclerotic changes were evident, and the basilar artery was not visualized at MR angiography. The posterior cerebral arteries were demonstrated via the posterior communicating arteries. Symmetrical infarctions of the paired AICA territories usually cause total involvement of the MCPs, including their surface, and manifest as heterogeneous signal intensity on T1- and T2-weighted images with relatively small lesions within the pons (22). Bilateral MCP infarction can occur in systemic lupus erythematosus (23). Isolated bilateral MCP infarction has been reported in a patient with vertebral artery dissection after head trauma (24).

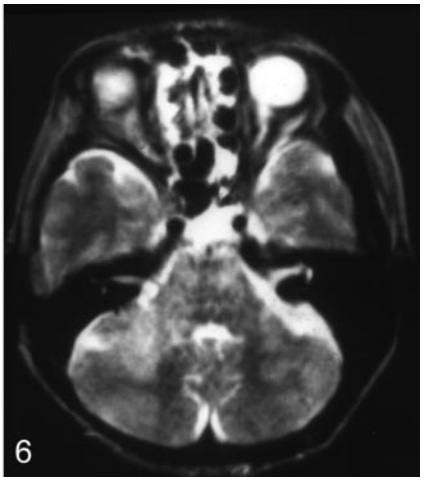

FIG 5. A 57-year-old man with bilateral MCP infarction. T2-weighted FSE MR image (3,600/102/2) shows bilateral hyperintensity in both MCPs. Also demonstrated are additional cerebellar infarction in the left AICA distribution and lacunar infarctions in the pons.

FIG 6. A 55-year-old woman with diffuse infiltrating B-cell malignant lymphoma. T2-weighted SE image (3,000/90/1) shows a heterogeneous hyperintensity extending from the pons into the cerebellar white matter through the MCPs. The hyperintensity is asymmetrical. Enlargement of the pons and right MCP is demonstrated.

Wallerian degeneration of the pontocerebellar tracts after pontine hemorrhage or pontine infarction causes bilateral symmetrical hyperintense signals in the MCPs on T2-weighted MR images and mild cerebellar atrophy. These hyperintensities are first recognized from 26 days to 4.5 months after hemorrhage and become undetectable 5 years after hemorrhage (22).

Hypertensive encephalopathy is an acute disorder that occurs in patients, with a dramatic rise in blood pressure associated with central nervous system (CNS) signs such as headache, seizures, visual disturbances, and altered mental status. Neuroimaging features in hypertensive encephalopathy include diffuse or focal hyperintensity on T2-weighted images, predominantly in the supratentorial white matter, especially in occipital lobes, but the MCPs, brain stem, and cerebellum can be involved in addition to the basal ganglia (25–27). In most cases, the changes of hypertensive encephalopathy appear to represent reversible vasogenic edema (27). T2 hyperintensity was extensively distributed in the bilateral basal ganglia, thalami, and cerebellum in our hypertensive patient with acute renal failure. These lesions, however, resolved promptly without any sequelae after control of blood pressure and recovery of the renal function. The symptoms and imaging findings of hypertensive encephalopathy have been found to be remarkably similar, if not identical, to changes associated with a number of other acute illnesses, including eclampsia-preeclampsia, thrombocytopenic thrombotic purpura, porphyria, and hypertension-inducing treatments such as erythropoietin, blood transfusions, or immunosuppressants, particularly cyclosporin-A and tacrolimus (FK506), and high-dose corticosteroids as well as various chemotherapeutic agents (27, 28). The term "posterior reversible encephalopathy (or edema) syndrome," or PRES, is preferred as a more appropriate description of the syndrome (28). In our study, cyclosporin-A encephalopathy was seen in a patient with chronic myelocytic leukemia (CML). There was a possibility that the hyperintensity in both MCPs and cerebellum was caused by involvement of CML; however, the hyperintensity was not observed at the time of diagnosis and developed after the intravenous administration of cyclosporin-A with subsequent deterioration of her mental status and convulsion. The hyperintensity disappeared after discontinuation of cyclosporin-A with clinical improvement.

Neoplasms, Related Disease, and Hamartomas

Three cases of malignant neoplasms (brain stem glioma, malignant lymphoma, and meningeal carcinomatosis) showed bilateral hyperintensity in both MCPs. Although most cases in the present study demonstrated symmetrical hyperintensity, a case of primary B-cell-type large-cell lymphoma presented as a diffusely infiltrating disease and demonstrated asymmetrical and heterogeneous hyperintensity extending from the pons into the cerebellar white matter through the MCPs (Fig 6) (29). This case and a case of brain stem glioma showed enlargement of the pons with hyperintense lesions. Enlargement of the affected structures is usually seen in malignant neoplasms; however, enlargement was absent in a case of meningeal carcinomatosis (Fig 7B). Additional multiple small hyperintensities were seen on T2-weighted images in the brain stem, basal ganglia, thalamus, and periventricular white matter. These lesions were not demonstrated by an MR study obtained 5 months earlier (Fig 7C). An autopsy revealed widespread periventricular-associated tumor infiltration in the leptomeninges and subarachnoid space with multifocal infarcts in both MCPs, pons, basal ganglia, thalamus, and periventricular white matter, as reported elsewhere (30).

Lymphomatoid granulomatosis (LG) is an uncommon multisystem disease characterized by multifocal angiocentric angiodestructive lymphoreticular proliferative and granulomatous lesion. Diffuse T2 hyperintense lesions in both MCPs, cerebllar hemisphere, and cerebral white matter have been reported in a patient with LG (31). In the patient, multiple punctate and linear enhancements have also been demonstrated.

Hamartomas, foci of prolonged T2 without significant mass effect, are detected in patients with neurofibromatosis type 1, most frequently in the MCPs,

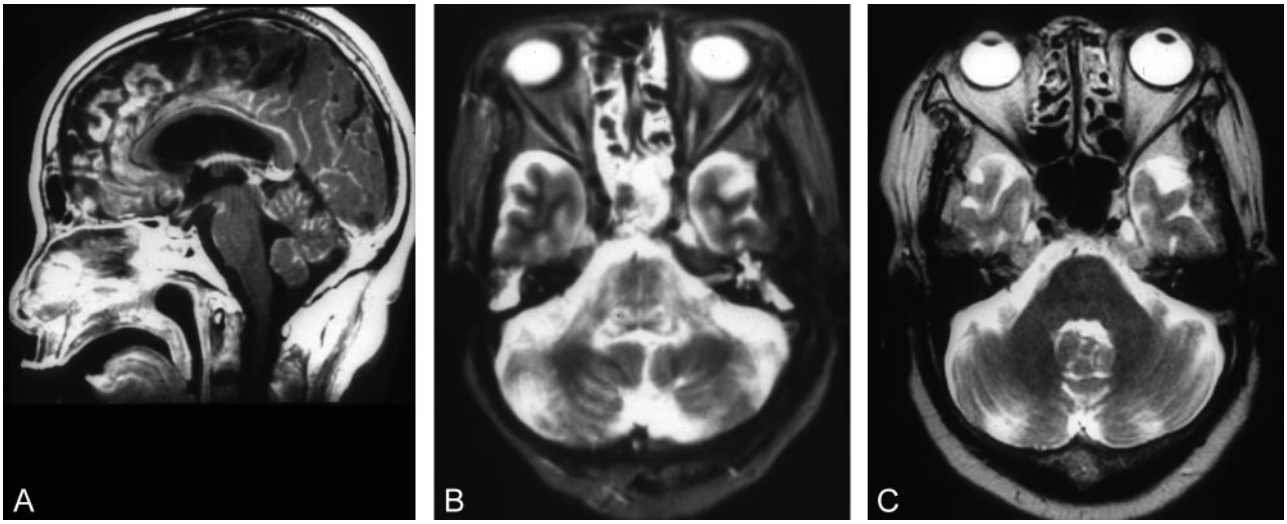

FIG 7. A 77-year-old woman with meningeal carcinomatosis. *A,* Postcontrast T1-weighted SE midsagittal image (600/15/1) shows enhancement in the cerebellar fissures and cortical sulci as well as the anterior margin of the midbrain and upper pons. *B,* T2-weighted FSE MR image (3,600/102/2) shows symmetrical hyperintensities of MCPs, upper cerebellar peduncles, lateral and dorsal pons. *C,* T2-weighted FSE MR image (3,600/102/2) obtained 5 months earlier showed no hyperintensities at the same level of that shown in *B.*

followed by the pons, globus pallidus, midbrain, thalamus, medulla oblongata, and, less frequently, the cerebral peduncles and cerebral white matter. Except for those in the globus pallidus, all of these foci are smaller than 1.5 cm and isointense relative to white matter on T1-weighted images (32). Bilateral, usually asymmetrical MCP hamartomas are observed in young patients without mass effect (32).

Demyelinating and Inflammatory Diseases

Bilateral hyperintensity of the MCPs was seen in demyelinating and inflammatory diseases, including MS, ADEM, Behçet disease, and HIV encephalopathy.

In many MS patients, T2 hyperintensities are most frequently present in the white matter adjacent to the trigones and bodies of the lateral ventricles. Confluent high signal intensity tends to occur around the frontal and occipital horns, often extending into the temporal lobes, and a high incidence of infratentorial lesions has been described elsewhere (33). Our MS patient showed mild cerebellar atrophy in addition to the characteristic T2 hyperintensities of the corpus callosum and the white matter adjacent to the lateral ventricles. Focal atrophy develops as a result of tissue damage or Wallerian degeneration (34).

ADEM is a monophasic immune reaction to a preceding viral infection or vaccination, and multifocal subcortical hyperintense foci are demonstrated on T2-weighted images. The lesions in ADEM involve the cerebral or cerebellar cortices, deep white matter, and brain stem (35, 36). Bilateral MCP involvement has been demonstrated elsewhere (36).

Behçet disease is a multisystem vasculitis of unknown etiology. Disseminated CNS disease predominantly involving the infratentorial white matter is seen in about 20–30% of patients (37). Although it may be difficult to differentiate MS from Behçet disease on the basis of MR findings (37, 38), the dominant involvement of the upper brain stem and diencephalic structure in Behçet disease has been observed (38). Pontine tegmentum can be affected, but the central part of the pons and the corticospinal tract are commonly involved in Behçet disease. Involvement of the basal ganglia, thalamus, and internal capsule and the absence of periventricular predominance of white matter lesions favor a diagnosis of Behçet disease (37, 38).

In HIV patients, multifocal confluent lesions or diffuse symmetric high signal intensity in the periventricular and deep white matter typically accompanies progression of disease. Bilateral symmetric increased signal intensity on T2-weighted images has been described in the basal ganglia and thalamus and may also involve the brain stem and the MCPs (39). In our HIV encephalopathy patient, hyperintensities in the pons, MCPs and frontal white matter regressed with antiretrovirus therapy with mild progression of brain atrophy. Symmetrical MCP involvement has been demonstrated in progressive multifocal leukoencephalopathy in an AIDS patient (39).

Central pontine myelinolysis (CPM) is characterized by regions of demyelination throughout the brain, but these regions are most prominent in the pons. The original patients studied were all chronic alcoholics, but subsequently the condition has been found in children and in other patients with electrolyte abnormalities, most notably hyponatremia, which had been corrected rapidly (40). In this study, there were two cases of CPM with typical pontine lesions. Both patients showed no MCP lesions, but symmetrical extension of a pontine lesion into bilateral MCPs has been reported elsewhere (40). In listerial rhombencephalitis, symmetrical MCP lesions have been demonstrated (41, 42).

Subacute sclerosing panencephalitis (SSPE) is a rare, progressive, inflammatory disease of the CNS

caused by persistent measles virus infection. The areas most commonly involved are the periventricular and subcortical white matter. Atrophy may accompany the white matter lesions. The basal ganglia, cerebellum, spinal cord, and corpus callosum are less commonly involved. Rarely, predominant involvement of the brain stem occurs with bilateral MCP lesions. A peculiar pattern, with involvement of the pons with extension to both MCPs and substantia nigra but sparing the pontine tegmentum, is suggested (43). The "cross sign" hyperintensity has been demonstrated in the pons in a patient with SSPE without atrophic change of the posterior fossa structures (43). Hyperintensity of both MCPs is not necessarily symmetrical in inflammatory and demyelinating diseases, but most cases showed symmetrical lesions in the present study.

Intoxication

Chronic solvent abuse, especially of pure toluene, can cause the symmetrical hyperintensity of both MCPs as well as white matter hyperintensities in cerebrum, brain stem, and cerebellum on T2-weighted MR images (44). White matter change on T2-weighted images is considered to represent damage to myelin, such as demyelination or myelin pallor. Gliosis may be related to these changes (44).

Bilateral symmetric high signal intensity of MCPs and pons on T2-weighted and fluid-attenuated inversion recovery images has been reported in patients with heroin inhalation toxicity (45). Symmetric involvement of the cerebellar white matter and posterior limb of the internal capsule, with sparing of the anterior limb and subcortical white matter, is characteristic, although involvement may be more extensive, depending on the severity of the condition. Symmetric spongiform degeneration occurs, particularly in the cerebral and cerebellar white matter and in corticospinal and solitary tracts (46).

In our study, both MCPs were spared in two patients with hemolytic-uremic syndrome involving the bilateral basal ganglia, pontine tegmentum, and cerebellum, as well as upper cerebellar peduncles (47–49). Lesions in the cerebellar white matter and in the dorsal part of the brain stem are observed in children with acute encephalopathy associated with viral infection (50) and in neonates with maple syrup urine disease (51). The pons can be affected in Japanese encephalitis (52), and similarities of MR findings between Japanese encephalitis and Wilson disease have also been reported (53), although MCP involvement has not been described in these diseases.

Recently, involvement of the MCP has been documented in Whipple disease (54). The disease is a systemic disorder affecting particularly the small bowel and inducing a malabsorption syndrome and is caused by a Gram-positive bacillus, *Tropheryma whippelii.* Osteoarticular, cardiac, and CNS involvements are also common (54). Bilateral lesions might occur in this disease, but we did not find any cases of MR-demonstrated bilateral MCP involvement.

Conclusion

Bilateral involvement of the MCPs is encountered in various pathologic conditions. Both MCPs can be affected, manifesting as degeneration of transverse pontocerebellar fibers, as a part of diffuse white matter lesion, or as continuous spread of the lesion from the pons. In some metabolic, demyelinating, and inflammatory diseases, the MCPs are preferentially affected, although the reason is unclear. Clinical and other MR features can suggest the diagnosis or help in narrowing the differential diagnosis.

References

1. Clemente CD, ed. *Gray's anatomy.* 30th ed. Philadelphia: Lea & Febiger, 1985;981–982
2. Savoiardo M, Strada L, Girotti F, et al. **Olivopontocerebellar atrophy: MR diagnosis and relationship to multisystem atrophy.** *Radiology* 1990;174:693–696
3. Naka H, Ohshita T, Murata Y, et al. **Characteristic MRI findings in multiple system atrophy: comparison of the three subtypes.** *Neuroradiology* 2002;44:204–209
4. Bürk K, Abele M, Fetter M, et al. **Autosomal dominant cerebellar ataxia type I: clinical features and MRI in families with SCA1, SCA2, and SCA3.** *Brain* 1996;119:1497–1505
5. Bürk K, Skalej M, Dichgans J. **Pontine MRI hyperintensities ("the cross sign") are not pathognomonic for multiple system atrophy (MSA).** *Mov Disord* 2001;16:535–536
6. Sugawara M, Toyoshima I, Wada C, et al. **Pontine atrophy in spinocerebellar ataxia type 6.** *Eur Neurol* 2000;43:17–22
7. Murata Y, Yamaguchi S, Kawakami H, et al. **Characteristic magnetic resonance imaging findings in Machado-Joseph disease.** *Arch Neurol* 1998;55:33–37
8. Imon Y, Katayama S, Kawakami H, et al. **A necropsied case of Machado-Joseph disease with a hyperintense signal of transverse pontine fibers on long TR sequences of magnetic resonance images.** *J Neurol Neurosurg Psychiatry* 1998;64:140–141
9. Uyama E, Kondo I, Uchino M, et al. **Dentatorubral-pallidoluysian atrophy (DRPLA): clinical, genetic, and neuroradiologic studies in a family.** *J Neurol Sci* 1995;130:146–153
10. Kumar AJ, Köhler W, Kruse B, et al. **MR findings in adult-onset adrenoleukodystrophy.** *AJNR Am J Neuroradiol* 1995;16:1227–1237
11. van Wassenaer-van Hall HN, van den Heuvel AG, Algra A, Hoogenraad TU, Mali WPTM. **Wilson disease: findings at MR imaging and CT of the brain with clinical correlation.** *Radiology* 1996;198:531–536
12. King AD, Walshe JM, Kendall BE, et al. **Cranial MR imaging in Wilson's disease.** *AJR Am J Roentgenol* 1996;167:1597–1584
13. Hanner JS, Li KCP, Davis GL. **Acquired hepatocerebral degeneration: MR similarity with Wilson disease.** *J Comput Assist Tomogr* 1988;12:1076–1077
14. Uchino A, Miyoshi T, Ohno M. **Case report: MR imaging of chronic persistent hepatic encephalopathy.** *Radiat Med* 1989;7:257–260
15. Inoue E, Hori S, Narumi Y, et al. **Portal-systemic encephalopathy: presence of basal ganglia lesions with high signal intensity on MR images.** *Radiology* 1991;179:551–555
16. Fujiioka M, Okuchi K, Hiramatsu K, et al. **Specific changes in human brain after hypoglycemic injury.** *Stroke* 1997;28:584–587
17. Boeve BF, Bell DG, Noseworthy JH. **Bilateral temporal lobe MRI changes in uncomplicated hypoglycemic coma.** *Can J Neurol Sci* 1995;22:56–58
18. Finelli PF. **Diffusion-weighted MR in hypoglycemic coma.** *Neurology* 2001;57:933–935
19. Mugikura S, Takahashi S, Higano S, et al. **MR findings in Tay-Sachs disease.** *J Comput Assist Tomogr* 1996;20:551–555
20. Cormier PJ, Long ER, Russell EJ. **MR imaging of posterior fossa infarctions: vascular territories and clinical correlates.** *Radiographics* 1992;12:1079–1096
21. Milandre L, Rumeau C, Sangla I, et al. **Infarction in the territory of the anterior inferior cerebellar artery: report of five cases.** *Neuroradiology* 1992;34:500–503
22. O'uchi T. **Wallerian degeneration of the pontocerebellar tracts after pontine hemorrhage.** *Int J Neuroradiol* 1998;4:171–177
23. Kwon SU, Koh JY, Kim JS. **Vertebrobasilar artery territory infarc-**

tion as an initial manifestation of systemic lupus erythematosus. *Clin Neurol Neurosurg* 1999;101:62–67
24. Akiyama K, Takizawa S, Tokuoka K, et al. **Bilateral middle cerebellar peduncle infarction caused by traumatic vertebral artery dissection.** *Neurology* 2001;56:693–694
25. de Seze J, Mastain B, Stojkovic T, et al. **Unusual MR findings of the brain stem in arterial hypertension.** *AJNR Am J Neuroradiol* 2000; 21:391–394
26. Weingarten K, Barbut D, Filippi C, Zimmerman RD. **Acute hypertensive encephalopathy: findings on spin-echo and gradient-echo MR imaging.** *AJR Am J Roentgenol* 1994;162:665–670
27. Morello F, Marino A, Cigolini M, Cappellari F. **Hypertensive brain stem encephalopathy: clinically silent massive edema of the pons.** *Neurol Sci* 2001;22:317–320
28. Casey SO, Truwit CL. **Pontine reversible edema: a newly recognized imaging variant of hypertensive encephalopathy?** *AJNR Am J Neuroradiol* 2000;21:243–245
29. Furusawa T, Okamoto K, Ito J, et al. **Primary central nervous system lymphoma presenting as diffuse cerebral infiltration.** *Radiat Med* 1998;16:137–140
30. Klein P, Haley EC, Wooten GF, Vandenberg SR. **Focal cerebral infarctions associated with perivascular tumor infiltrates in carcinomatous leptomeningeal metastases.** *Arch Neurol* 1989;46:1149–1152
31. Tateishi U, Terae S, Ogata A, et al. **MR Imaging of the brain in lymphomatoid granulomatosis.** *AJNR Am J Neuroradiol* 2001;22: 1283–1290
32. Aoki S, Barkovich AJ, Nishimura K, et al. **Neurofibromatosis type 1 and 2: cranial MR findings.** *Radiology* 1989;172:527–534
33. Fazekas F, Offenbacher H, Fuchs S, et al. **Criteria for an increased specificity of MRI interpretation in elderly subjects with suspected multiple sclerosis.** *Neurology* 1988;38:1822–1825
34. Falini A, Kesavadas C, Pontesilli S, et al. **Differential diagnosis of posterior fossa multiple sclerosis lesions: neuroradiological aspects.** *Neurol Sci* 2001;22[suppl]:S79–S83
35. Singh S, Alexander M, Korah IP. **Acute disseminated encephalomyelitis: MR imaging features.** *AJR Am J Roentgenol* 1999;173: 1101–1107
36. Khong P-L, Ho H-K, Cheng P-W, et al. **Childhood acute disseminated encephalomyelitis: the role of brain and spinal cord MRI.** *Pediatr Radiol* 2002;32:59–66
37. Lee SH, Yoon PH, Park SJ, Kim DI. **MRI findings in neuro-Behçet disease.** *Clin Radiol* 2001;56:485–494
38. Koçer N, Islak C, Siva A, et al. **CNS involvement in neuro-Behçet syndrome: an MR study.** *AJNR Am J Neuroradiol* 1999;20:1015–1024
39. Nusbaum AO, Fung K-M, Atlas SW. **White matter diseases and inherited metabolic disorders.** In: Atlas SW, ed. *Magnetic resonance imaging of the brain and spine.* 3rd ed. Philadelphia: Lippincott Williams & Wilkins, 2002;457–563
40. Miller GM, Baker Jr HL, Okazaki H, Whisnant JP. **Central pontine myelinolysis and its imitators: MR findings.** *Radiology* 1988;168: 795–802
41. Soo MS, Tien RD, Gray L, Andrews PI, Friedman H. **Mesenrhombencephalitis: MR findings in nine patients.** *AJR Am J Roentgenol* 1993;160:1089–1093
42. Alper G, Knepper L, Kanal E. **MR findings in listerial rhombencephalitis.** *AJNR Am J Neuroradiol* 1996;17:593–596
43. Senol U, Haspolat S, Cevikol C, Saatci I. **Subacute sclerosing panencephalitis: brain stem involvement in a peculiar pattern.** *Neuroradiology* 2000;42:913–916
44. Yamanouchi N, Okada S, Kodama K, et al. **White matter changes caused by chronic solvent abuse.** *AJNR Am J Neuroradiol* 1995;16: 1643–1649
45. Keogh CF, Andrews GT, Spacey SD, et al. **Neuroimaging features of heroin inhalation toxicity: "chasing the dragon."** *AJR Am J Roentgenol* 2003;180:847–850
46. Wolters EC, van Wijngaarden GK, Stam FC, et al. **Leukoencephalopathy after inhaling heroin pyrolysate.** *Lancet* 1982;2:1233–1237
47. Sherwood JW, Wagle WA. **Hemolytic uremic syndrome: MR findings of CNS complications.** *AJNR Am J Neuroradiol* 1991;12:703–704
48. Hager A, Staudt M, Klare B, et al. **Hemolytic-uremic syndrome with involvement of basal ganglia and cerebellum.** *Neuropediatrics* 1999;30:210–213
49. Signorini E, Lucchi S, Mastrangelo M, et al. **Central nervous system involvement in a child with hemolytic uremic syndrome.** *Pediatr Nephrol* 2000;14:990–992
50. Yagishita A, Nakano I, Ushioda T, et al. **Acute encephalopathy with bilateral thalamotegmental involvement in infants and children: imaging and pathology findings.** *AJNR Am J Neuroradiol* 1995;16: 439–447
51. Brismar J, Aqeel A, Brismar G, et al. **Maple syrup urine disease: findings on CT and MR scans of the brain in 10 infants.** *AJNR Am J Neuroradiol* 1990;11:1219–1228
52. Kumar S, Misra UK, Kalita J, et al. **MRI in Japanese encephalitis.** *Neuroradiology* 1997;39:180–184
53. Saha M, Kumar S, Das A, Gupta RK. **Similarities and differences of MR findings between Japanese encephalitis and Wilson's disease.** *Eur Radiol* 2002;12:872–876
54. Kremer S, Besson G, Bonaz B, et al. **Diffuse lesions in the CNS revealed by MR imaging in a case of Whipple disease.** *AJNR Am J Neuroradiol* 2001;22:493–495